Failure Modes for Stiction in Surface-Micromachined MEMS[1]

Abhijeet Kolpekwar†, R.D.(Shawn) Blanton†, and David Woodilla‡

†ECE Department
Carnegie Mellon University
Pittsburgh, PA 15213-3890

‡Analog Devices
21 Osborn Street
Cambridge, MA 02139

ABSTRACT

Wafer-level testing of surface-micromachined sensors provides new challenges to the test community. Currently, there is no method available for performing direct measurements to assess faulty micromechanical structures. Most commercial methods use electrical measurements to deduce the physical source of failures in the micromechanical structure. As a result, the process of identifying various failure modes (electrical measurements) and accurately mapping them to the underlying physical failure mechanisms of the mechanical sensor becomes highly complex. Several sources of failures that include particulates and stiction complicate the situation even more. Here, we provide a case study of the Analog Devices ADXL75 Accelerometer. One failure category called stuck/tipped beams is investigated and a methodology is developed to uniquely distinguish failures either caused by stuck or tipped beams. The proposed method is easy to implement and the information obtained can be critical for yield improvement.

1 Introduction

Surface-micromachined MEMS is a class of MEMS devices where the micromechanical structure is fabricated using layers of thin films deposited on the substrate. Surface micromachining enables the fabrication of high-quality sensors and actuators as MEMS devices. Most commercial applications use surface micromachining because of its well developed infrastructure for depositing, patterning and etching thin films for silicon integrated circuit technology. Early application of this technology include the digital mirror display, which has a large number of aluminum thin-film mirrors fabricated on the top of a CMOS static random access memory (SRAM) [1]. Another popular product, which is discussed in this paper, is Analog Devices ADXL75 accelerometer. Figure 1 shows a die shot of the ADXL50, an open-loop predecessor of the ADXL75. Like the ADXL75, it uses a surface-micromachined microresonator to sense and convert an acceleration into a linearly-related voltage for triggering air-bag deployment in automobiles [2, 4, 3]. However, the ADXL75 utilizes a closed-loop system to prevent unconstrained microstructure movement.

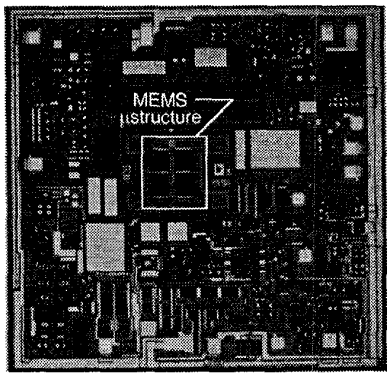

Figure 1: Die shot of the Analog Devices ADXL50 accelerometer.

Surface-micromachined microstructures typically range from 0.1 to several μm in thickness and 10 to 500 μm in length. A typical height of the "suspended" structure above the substrate is 1 μm. Thus, the large surface area and small offset from adjacent surfaces make these microstructures vulnerable to stiction. *Stiction* is the adhesion of the microstructure to adjacent surfaces. It can occur during the final steps of the micromachining process (where the structure is released) or after packaging of the device due to out-of-range input signals or electromechanical instability [5]. Thus, stiction is a source of yield loss during the fabrication of surface micromachined devices.

In this paper, we focus on techniques to identify a

[1]This research effort is sponsored by the National Science Foundation under grant MIP-9702678 and the Defense Research Projects Agency under Rome Laboratory, Air Force Materiel Command, USAF, under grant F30602-97-2-0323.

failure mode (i.e. an electrical measurement) to distinguish between the two most common physical failure mechanisms occurring due to stiction: *tipped* beams and *stuck* beams. Figure 2 illustrates both stuck and tipped beams. Stuck beams get stuck down (flat) on the substrate because of the strong adhesive forces resulting from surface interactions. Stuck beams show no movement since they are virtually anchored to the substrate. Tipped beams, on the other hand, are tilted out of line in the x, y, and z directions. These beams can also exhibit a high degree of curvature. In this case, adhesive forces are not strong enough to force the beam completely to the surface. Thus, tipped beams can exhibit some degree of movement. Figure 2c shows a beam tipped down towards the surface. Differentiation between these two modes of failure is important for yield improvement. This paper presents one methodology for distinguishing these failure types.

The remaining parts of this paper are organized as follows: Section 2 describes the operational basics of the accelerometer. Section 3 discusses the spectrum analysis and forward gain measurement for the accelerometer and their use in failure analysis. Section 4 states our experiments and the results obtained. Finally, Section 5 presents our conclusions.

2 Accelerometer Operation

Figure 3 illustrates the basic sensing operation of a typical accelerometer. The micromechanical structure of the accelerometer consists of a shuttle mass that is designed to move with respect to its package under an applied acceleration. There is an array of parallel beams attached to both sides of the shuttle mass. (For the purposes of simplicity, we have only shown one side of beams in Figure 3.) Between every pair of fixed beams is a moving beam. Such an arrangement of fixed and movable beams produces an array of differential parallel-plate capacitors. The capacitance C, for every pair of moving-fixed parallel beams is given by the simple equation:

$$C = \frac{A\epsilon}{d} \qquad (1)$$

where A is the area of parallel plates (i.e. beam overlap), ϵ is the permitivity of the space between the beams and d is the distance between parallel beams.

Thus, when the shuttle moves in the y direction as shown in Figure 3b, the distance d between the parallel beams changes, resulting in a corresponding change in the capacitance. Observe in Figure 3b, the capacitance for one pair of parallel beams increases to $C + \Delta C$ and decreases for the other pair to $C - \Delta C$.

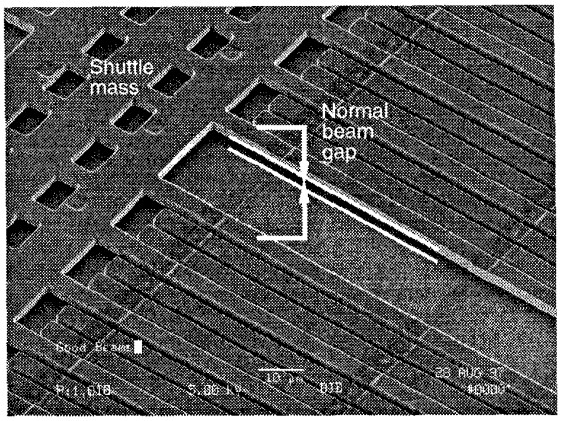

(a)

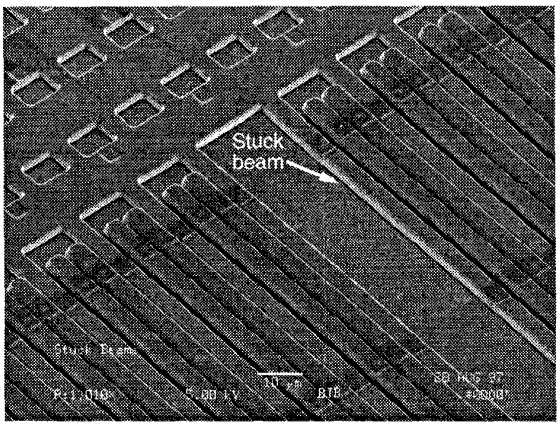

(b)

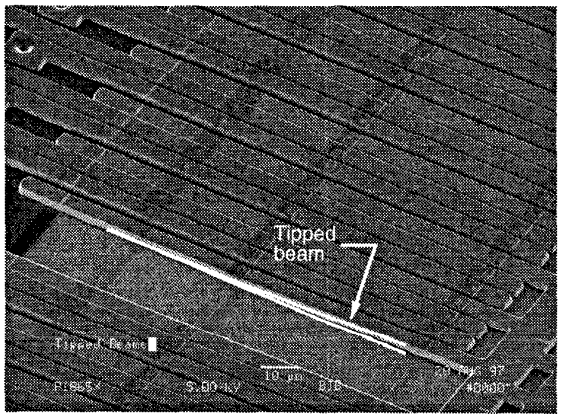

(c)

Figure 2: Effect of stiction on surface-micromachined accelerometer: (a) A defect-free accelerometer; (b) an accelerometer with stuck-down beams; and (c) an accelerometer with a tipped beam.

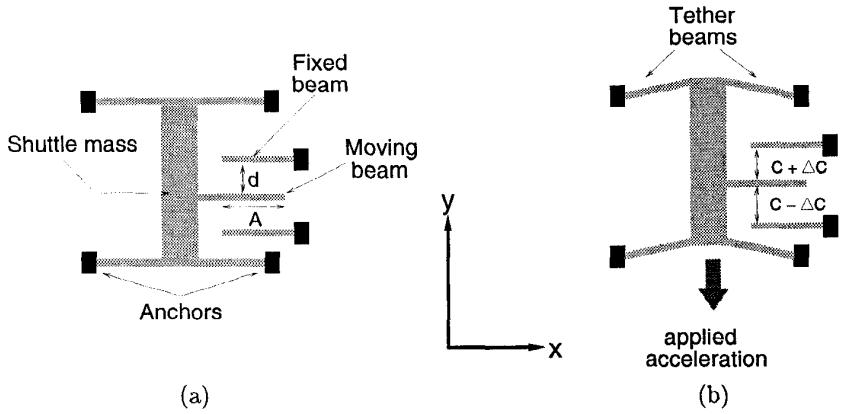

Figure 3: Sensing operation of a typical accelerometer: (a) Microresonator shuttle at rest and (b) under an applied acceleration.

Similarly, if the shuttle moves in the x-direction, area A of the beam overlap changes which results in a change of capacitance. Thus, shuttle movement can be converted to an equivalent change in capacitance. A circuit for sensing the capacitance change is shown in Figure 4. This circuit senses and converts a capacitance change to a linearly-related change in output voltage. Two square waves of the same amplitude but 180° out of phase are applied to the potential divider arrangement. Initially, when the shuttle is stationary, the opposite voltages applied to the fixed beams produce a zero-volt output. However, with the slightest shuttle movement, the capacitance balance is disturbed and a non-zero output voltage V_b results. A demodulator then uses V_b to produce a DC voltage V_{dem} representing the magnitude and direction (+ or −) of the acceleration. The demodulator uses one of the signals driving the potential divider arrangement as a reference voltage.

In summary, the shuttle mass senses acceleration and converts it to a corresponding change in the differential capacitance. Sensing circuitry then converts this capacitance change to an equivalent change in voltage. This is the basic principle behind accelerometer operation.

As shown in Figure 1, a typical accelerometer consists of a microresonator and some surrounding electrical circuitry. There are three distinct components of the microresonator: The *shuttle* is a proof mass that moves under acceleration, the *combs* are the parallel beams (fixed and movable) that form differential capacitances and the long, thin *tether* beams are used to apply a restoring force to the displaced shuttle. The stiction problem discussed in the earlier section can affect all these beams in various ways. Hence, the comb and tether beams can become stuck and tipped.

3 Accelerometer Failure Modes

In this section, we discuss the electrical measurements used to assess the defective micromechanical structure in the accelerometer. The goal here is to identify a failure mode (an electrical measurement) that obtains as much information as possible about the tipped/stuck beam phenomenon. The failure modes discussed are obtained at the wafer level.

3.1 Frequency Analysis

Analysis of microresonator's frequency spectrum can reveal pertinent information about the microstructure. Thus, microresonator frequency can be used as a important failure mode for accelerometers.

Resonant frequency of the resonator is given by:

$$f_o = \frac{1}{2\pi}\sqrt{\frac{k}{m}} \tag{2}$$

where m is the shuttle mass and k is the spring constant provided by the tether beams. Using force balance,

$$ma = kx \tag{3}$$

where a is the applied acceleration and x is the shuttle movement. Using equations 2 and 3 gives

$$\frac{x}{a} = \frac{1}{4\pi^2 f_o^2} \tag{4}$$

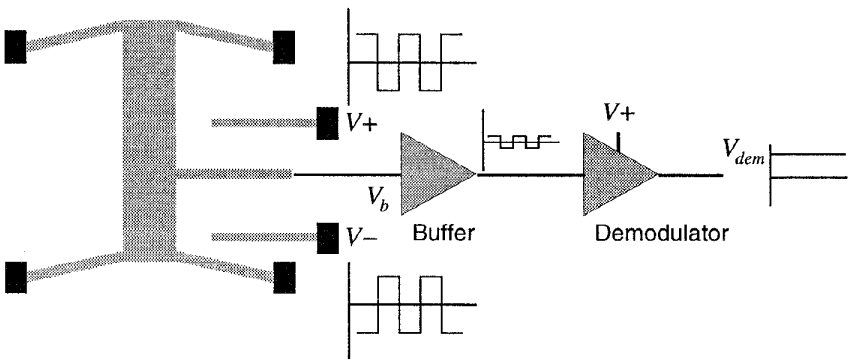

Figure 4: Signal conditioning operation of a typical accelerometer.

Thus, f_o can be obtained via the measurement of shuttle movement sensitivity to acceleration.

The frequency spectrum for the accelerometer can be generated by exciting the beams using a $sin(x)/x$ input waveform. The bandwidth of the waveform is determined using parameters of the accelerometer design and the expected resonant frequency of the microresonator. The beams are excited using this waveform and the accelerometer response voltage is measured. The frequency spectrum is then generated as a plot of output voltage versus frequency.

The two important parameters used in frequency spectrum analysis are 3-dB bandwidth (F_{3dB}) and the quality factor Q. F_{3dB} is the frequency range between f_l and f_h, where f_l and f_h are the frequencies below and above the resonant frequency f_o for which the gain A of the device is reduced by 3 dB to A_{3db}. (See Figure 5a.) Q is a measure of the sharpness of the 3-db bandwidth. Higher Q values imply a sharper resonant peak. Q is given by:

$$Q = \frac{f_o}{F_{3dB}} \tag{5}$$

Failures in the accelerometer can affect f_o, F_{3dB} and Q. These failure types can be mapped to the underlying physical source to a fairly good extent.

- **f_o failures:** Figure 5a shows a frequency spectrum of a fault-free resonator. The spectrum clearly shows the presence of a resonant peak at f_o. Figure 5b shows the spectrum for a resonator affected by tipped or stuck beams. This faulty spectrum is flat for both cases of the stiction problem. This means resonator movement is either impeded due to tipped beams or is completely absent because of stuck beams. However,

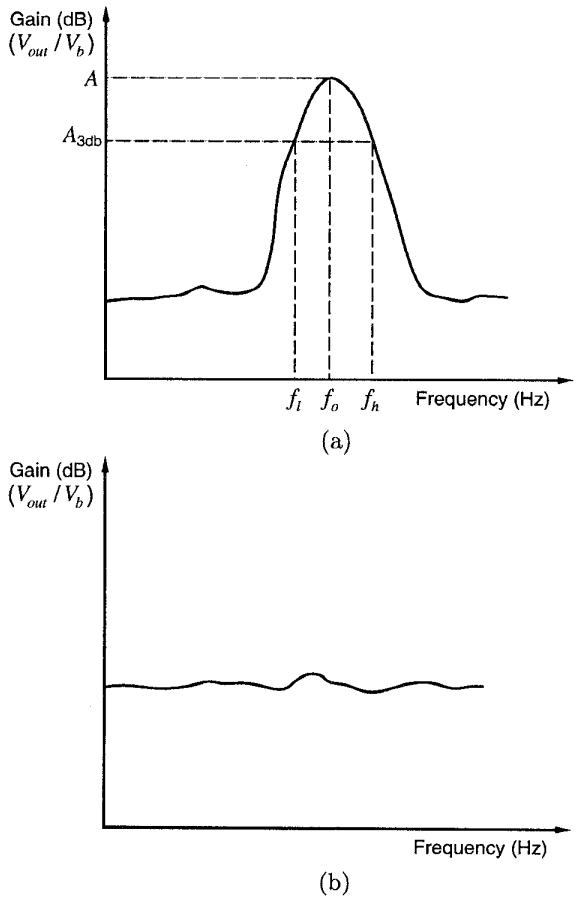

Figure 5: Frequency spectrums for accelerometers: (a) Fault-free case and (b) case for stuck or tipped beams.

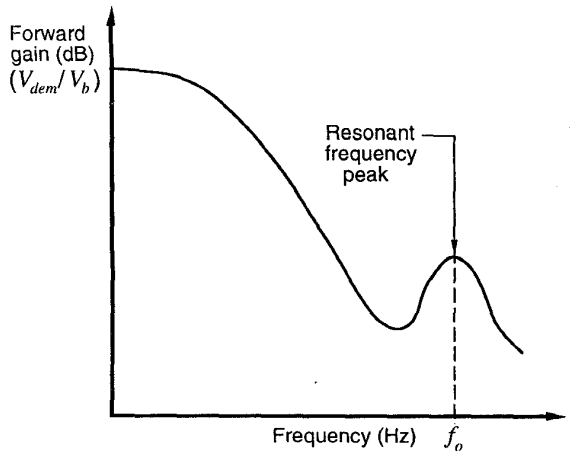

Figure 6: Typical frequency transfer characteristic of forward gain G.

the faulty spectrum gives no clear indication of the failure source (stuck or tipped beams). In general, absence of any resonant frequency in the spectrum shows that the beams are vibrationally challenged. This means beam movement is insufficient to meet the desired functionality.

- **F_{3dB} and Q failures:** High F_{3dB} failures (or low Q failures) indicate an absence of any sharp frequency peak in the spectrum. This is generally caused by impaired or stuck beams. Low F_{3dB} failures (or high Q failures) indicate the presence of noise spikes in the spectrum. This suggests that electrical noise interfered with the test and there is no strong natural frequency signal. However, these failures cannot be directly mapped to the source of the beam failures. The beams may show a natural frequency peak that may remain undetected due to noise in the spectrum. So, these failure modes have a limited capability for accurately predicting the nature of the defective microstructure.

3.2 Forward Gain Measurement

Measurement of forward gain can be used to effectively analyze the defective microstructure. It is a crucial factor in determining the sensitivity (volts/g) of the accelerometer. Forward gain G is defined as

$$G = \frac{V_{dem}}{V_b} \tag{6}$$

where V_{dem} is the demodulator voltage and V_b is the comb beam voltage as described before. The demodulator uses one of the input square waves (applied to the combs initially) as a reference. The main function of a demodulator is to produce a DC voltage representing the magnitude and direction of the differential acceleration signal detected. Typical frequency transfer characteristics of V_{dem}/V_b obtained using a dynamic signal analyzer are shown in Figure 6.

Forward gain is strongly dependent on the finger capacitance which in turn depends on the area of the fingers and the beam gap. Thus, failure modes of the forward gain are closely related to the physical characteristics of the beams. Failure on the forward gain could also be mapped to circuitry problems with the demodulator gain. But probability of this occurring is negligible when compared to the likelihood of stuck or tipped beams. High forward gain (failure above f_o) typically indicates that beams are not stuck. Failure on the low side (below f_o) could be due to stuck/tipped beam problems or beam gaps that are too wide.

4 Experimental Results

Experiments were performed at Analog Devices using ADXL75 accelerometer wafers. Our objective was to distinguish between tipped and stuck beams using spectrum analysis and forward gain measurement. In this section, we present our findings and the intuitive reasoning behind the observations.

Spectrum parameters and forward gain for 80 different dice were measured from five different fabrication lots of ADXL75 wafers. The resonant frequency for the fault-free ADXL75 is about 24 KHz and the forward gain is allowed to vary between -0.7 dB and -0.05 dB [6].

Our findings show that spectrum-related failure modes are very difficult to identify. A significant amount of time is required to generate the spectrum and to locate the resonance peak. Spectrums generated for ADXL75 have a significant amount of noise present. Hence, obtaining a good spectrum requires several runs to be averaged. This, of course, requires extra processing time for acquiring and averaging more test data. A quadratic curve fit algorithm is used to locate the spectrum peak. This approach is both computationally and memory intensive due to the need to store and manipulate the spectrum data. In addition, information provided by the algorithm does not help to distinguish stuck and tipped beams. Moreover, inaccurate thresholds for curve fits may reject good spectrums (yield loss) or accept bad ones (defect escape). We also observed that the complex process of spectrum generation may lead to poor spectrums even for defect-free accelerometers. Hence, the

Beam defect	Forward gain (G)
Tipped	$0.01 \leq \|G\| \leq 0.09$
Stuck	$\|G\| \leq 0.009$

Table 1: Forward gain failure modes for stuck and tipped beams.

parameters extracted from the spectrum analysis may be misleading and cause incorrect conclusions. Thus, spectrum-related parameters do not contribute to the identification of the source of stiction.

The results of the forward gain measurements, on the other hand, are more beneficial. The forward gain values obtained on the 80 dice indicated a clear distinction between the tipped and the stuck beams. The observations listed in Table 1 held true irrespective of the outcome of spectrum-related tests. In the case of tipped beams, there is some finger overlap which leads to an appreciable value of finger capacitance resulting in a small ($0.01 \leq |G| \leq 0.09$) forward gain. In the case of stuck beams, the amount of finger overlap is negligible which results in a minute finger capacitance with a forward gain of less than -0.009. In the case of broken (but not stuck) fingers, the capacitance is very low because of the absence of some comb fingers. This leads to a small value of forward gain as well. Thus, the forward gain measurement gives a clear indication of the source of the physical failure.

Some of the dice with tipped beams were manually "pushed" down to make them stuck down. It was observed that G decreases by an order of magnitude due to pushing. This confirmed our hypothesis even further. Beam curvatures were also measured to confirm our observations about tipped/stuck beams. Based on these observations, the following test changes were suggested to enhance the ADXL75 testing process.

- **Test sequence modification:** Performing spectrum tests before forward gain measurement can be a waste of time since computed spectrum parameters can be misleading. Performing forward gain measurement before spectrum analysis will not only save test time but will distinguish tipped beams from stuck ones.
- **Roll-off at 3-dB frequencies:** *Roll off* is the slope of the spectrum at the 3-dB frequency points. This value can be effectively used to distinguish a noisy spectrum from a noise-free one. Very high values of roll-off can indicate noisy spectrums. For stuck/tipped beams, the computed roll off values were found to be very high (more than 1dB/100Hz), mainly due to the noisy spectrums.
- **Beam curvature versus forward gain:** It may be possible to find an empirical relationship between beam curvature and forward gain since forward gain is very sensitive to the beam curvature. However, this will require a significant amount of data collection to generalize these observations.

5 Conclusion

Our observations show that forward gain can be effectively used as a parameter to differentiate between tipped and stuck-beam failures for comb-drive accelerometers. Experiments with the Analog ADXL75 accelerometer indicate that forward gain values resulting from wider beam gaps are usually higher than the acceptable range. We hypothesize that performing forward gain measurement before the spectrum analysis will definitely improve the test quality of comb-drive accelerometers.

References

[1] L.J.Hornbeck, "Current Status of the Digital Micromirror Device (DMD) for Projection Television Application", In the *Proc. on International Electron Devices Meeting,* Washington, D.C., 1993.

[2] R.S. Payne, S. Sherman, S. Lewis and R.T. Howe, "Surface Micromachining: From Vision to Reality to Vision (accelerometer)", In the *Proc. on International Solid State Circuits Conference,* pp. 164-165, San Francisco, CA, 1995.

[3] L. Zimmermann, "Airbag Application: A Microsystem Including a Silicon Capacitive Accelerometer, CMOS Switched-Capacitor Electronics and True Self-Test Capability", *Sensors and actuators A 46-47,* pp. 190-195, 1995.

[4] T. Core, R. S. Payne, D. Quinn, S. Sherman and W. K. Wong, "Integrated Complete, Affordable Accelerometer for Air-Bag Applications", In the *Proc. of Sensors Expo,* pp. 240-241, Chicago IL, 1991.

[5] R. Maboudian and R.T. Howe, "Critical Review: Stiction in Surface Micromechanical Structures", *Journal of Vacuum Science and Technology B (Microelectronics and Nanometer Structures),* Vol. 15, No. 1, pp. 1-20, Jan. 1997.

[6] Analog Devices, *Accelerometer Data Sheets,* Application Notes and Worldwide Sales Directory.